VOLUME 241 (8) AUGUST 2011 ISSN 0029-5493

Nuclear Engineering and Design

An International Journal devoted to all aspects of Nuclear Fission Energy

CONTENTS

(Contents continued on back cover)

Available online at ScienceDirect
www.sciencedirect.com

Affiliated with the European Nuclear Society (ENS) and with the International Association for Structural Mechanics in Reactor Technology, e.V. (IASMiRT)

Nuclear Engineering and Design 241 (2011) 2859–2864

Contents lists available at ScienceDirect

Nuclear Engineering and Design

journal homepage: www.elsevier.com/locate/nucengdes

Monte Carlo simulation of the thermal column and beam tube of the TRIGA Mark II research reactor

R. Khan*, S. Karimzadeh, T. Stummer, H. Böck

Atominstitute (ATI), Vienna University of Technology (TU Wien), Stadion allee 2, A-1020 Vienna, Austria

ARTICLE INFO

Article history:
Received 4 December 2010
Received in revised form 13 April 2011
Accepted 14 April 2011

ABSTRACT

The Monet Carlo simulation of the TRIGA Mark II research reactor core has been performed employing the radiation transport computer code MCNP5. The model has been confirmed experimentally in the PhD research work at the Atominstitute (ATI) of the Vienna University of Technology. The MCNP model has been extended to complete biological shielding of the reactor including the thermal column, radiographic collimator and four beam tubes. This paper presents the MCNP simulated results in the thermal column and one of the beam tubes (beam tube A) of the reactor. To validate these theoretical results, thermal neutron flux density measurements using the gold foil activation method have been performed in the thermal column and beam tube A (BT-A). In the thermal column, the theoretical and experimental results are in fairly good agreement i.e. maximum thermal flux density in the centre decreases in radial direction. Further, it is also agreed that thermal flux densities in the lower part is greater than the upper part of the thermal column. In the BT-A experiment, the thermal flux density distribution is measured using gold foil. The experimental and theoretical diffusion lengths have been determined as 10.77 cm and 9.36 cm respectively with only 13% difference, reflecting good agreement between the experimental and simulated results. To save the computational cost and to incorporate the accurate and complete information of each individual Monte Carlo MC particle tracks, the surface source writing capability of MCNP has been utilized to the TRIGA shielding model. The variance reduction techniques have been applied to improve the statistics of the problem and to save computational efforts.

1. Introduction

Atominstitute has been operating the TRIGA Mark II research reactor since March 1962 with a thermal power of 250 kW. It has a completely mixed core of three types of fuel elements. This reactor is the only operating nuclear research facility in Austria (Böck, 1996). Since its first operation, this reactor has been serving five main purposes: (1) research and training in nuclear technology fields, (2) radio-isotope production for in-house research, (3) neutron scattering experiments to study neutron- and solid-state physics, (4) neutron radiography/tomography and (5) neutron activation analysis. The first two research areas are utilizing several irradiation facilities located inside the reactor core while the remaining three research fields are using the facilities outside the reactor core. This paper concentrates the neutronics analysis of the beam tube A and the a thermal column. Three of these beam tubes (A, B, and C) are radial while the fourth one is tangential. The top and side views of the reactor are shown in Figs. 1 and 2, respectively, where the reactor core, surrounding graphite reflector, four beam tubes, thermal column, radiographic collimator, reactor tank and biological TRIGA shielding can be seen (Khan, 2010).

1.1. Thermal column

The thermal column of the ATI reactor is a large, boral-lined, graphite-filled aluminum (Al) container with outside dimensions 1.2 m × 1.2 m in cross section and 1.6 m in depth. It is divided into two parts; the inner part is right at the peripheral of the annular graphite reflector, and the outer part is right behind the thermal column door. The aluminum container is opened toward the reactor room. Blocks of AGOT nuclear grade graphite occupy the entire void. The dimensions of each block are approximately 10.2 cm × 10.2 cm in cross-section and 127 cm in length. The door is filled with heavy aggregate concrete having density of 3.5 g/cm^3 (GA, 1962).

1.2. Beam tube A

To satisfy the experimental irradiation requirements outside the reactor core, there are four Beam tubes BT(s) i.e. A, B, C and D. Three of these BT(s) are radial while the fourth one (i.e. BT D) is tangential to the reactor core. All four BT(s) have the same radial dimensions i.e. 15.2 cm inner diameter. The top view of these BT(s) can be seen

* Corresponding author.
E-mail address: rustamzia@yahoo.com (R. Khan).

0029-5493/$ – see front matter © 2011 Elsevier B.V. All rights reserved.
doi:10.1016/j.nucengdes.2011.04.025

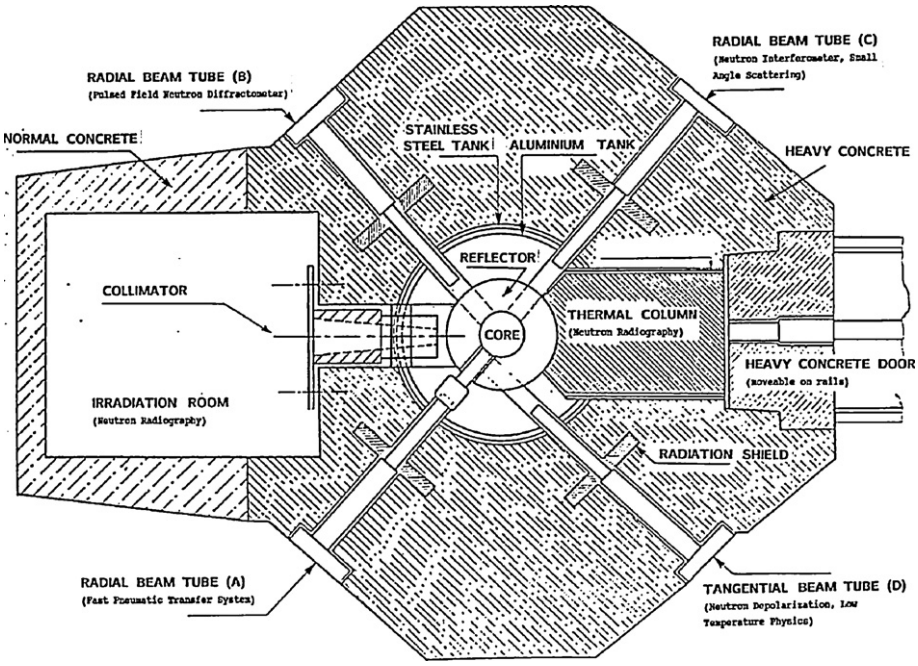

Fig. 1. Top view of the TRIGA Mark II research reactor.

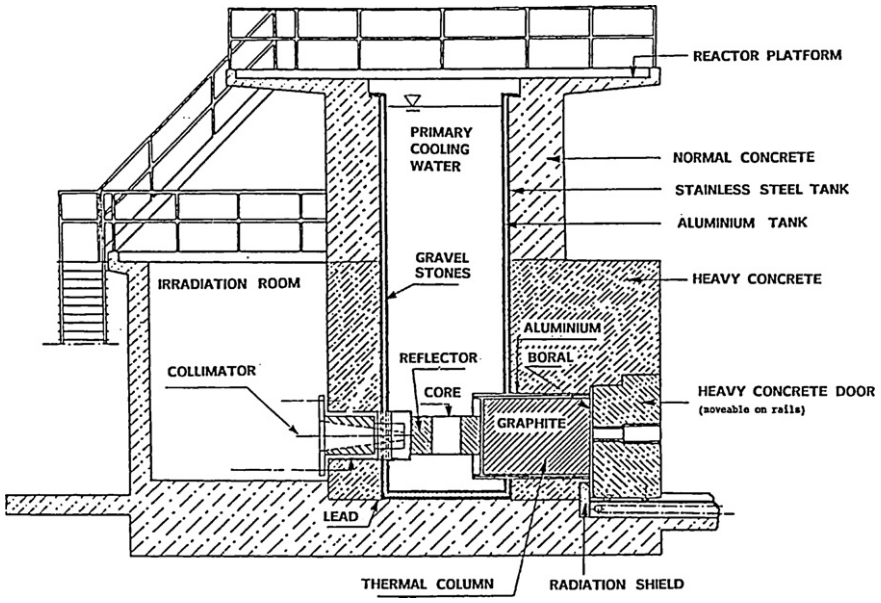

Fig. 2. Side view of the TRIGA Mark II research reactor.

in Fig. 1. The four BT(s) penetrate the concrete shield and the Al tank and pass through the reactor tank water to the reflector. These tubes provide neutron beams and gamma radiation for a variety of experiments. These tubes also provide the irradiation facilities for large specimens (up to 15 cm) in a region close to the core. Two of the radial tubes terminate at the outer edge of the reflector assembly but are aligned with the cylindrical void in the reflector graphite. The third (i.e. BT-A) tube, specifically developed for neutron activation, penetrates into the graphite reflector and terminates at the inner surface of the reflector, just at the outer edge of the core.

2. Experiments

2.1. Thermal column experiment

The thermal neutron flux measurement was performed in the thermal column of the TRIGA research reactor by using the gold foil method. Bare and cadmium-covered gold foils with a diameter of 5 mm and an average weight of 0.0084 g were used for this experiment at (Karimzadeh, 2004).

For this purpose the concrete door of the thermal column was opened and the foil detectors were installed in the thermal col-

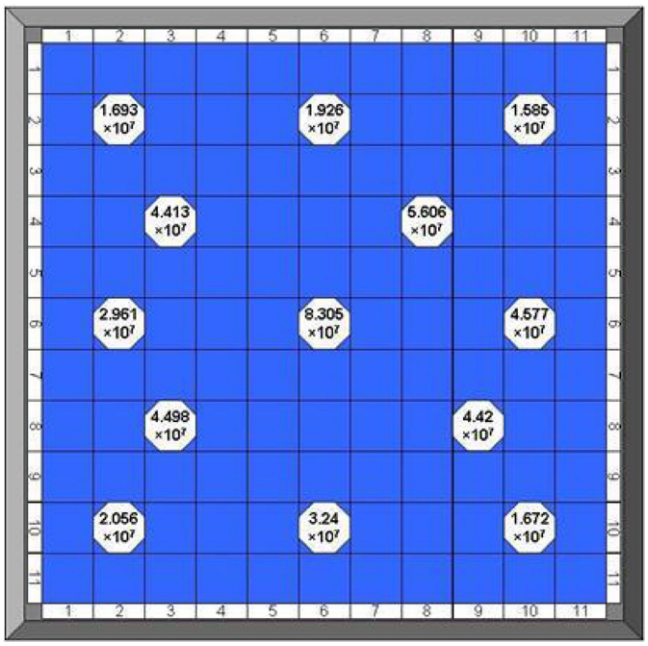

Fig. 3. Thermal neutron flux determination on the surface of the reactor thermal column.

Table 1
Neutron flux density distribution in the BT-A.

Positions (cm)	Total flux density	Flux density (≤0.4 eV)	Flux density (≥0.4 eV)
0	1.08E11	6.94E10	3.11E10
12	3.12E10	2.03E10	9.51E09
24	1.03E10	6.59E09	2.86E09
36	3.47E09	2.20E09	9.30E08
48	1.17E09	7.25E08	2.76E08
60	4.12E08	2.65E08	1.18E08

umn at 13 positions different positions. The air gap between the thermal column and the concrete door was about 2 cm. The reactor was operating at 250 kW and the gold foils (bare and Cd-covered) were irradiated for a duration of 10 min. After reactor-shutdown, the gold foils were removed and the activities were measured using a 4π beta counter system. The results of this experiment have been shown in Fig. 3 (Karimzadeh, 2004).

2.2. Beam tube-A experiment

The neutron measuring experiment using the gold foil activation method has been performed in BT-A on 28th March 2007 (Krejci, 2007). In this experiment, six gold foils (with and without cadmium cover) installed at each 12 cm were irradiated at a reactor power of 100 kW and measured using the barite concrete barrel of 60 cm length. The experimental results are given in Table 1.

3. Development of MCNP model

A detailed MCNP model of the ATI reactor has been developed (Khan, 2010) by using a 3-D continuous energy Monte Carlo code (MC team, 2005). This model uses continuous energy cross-section data and $S(\alpha, \beta)$ scattering functions from JEFF3.1. To perform the calculations outside the TRIGA core (e.g. at the thermal column and in any of the BT(s), the model is extended to the complete biological shielding including all four BT(s), radiographic collimator and thermal column as shown in Figs. 4 and 5.

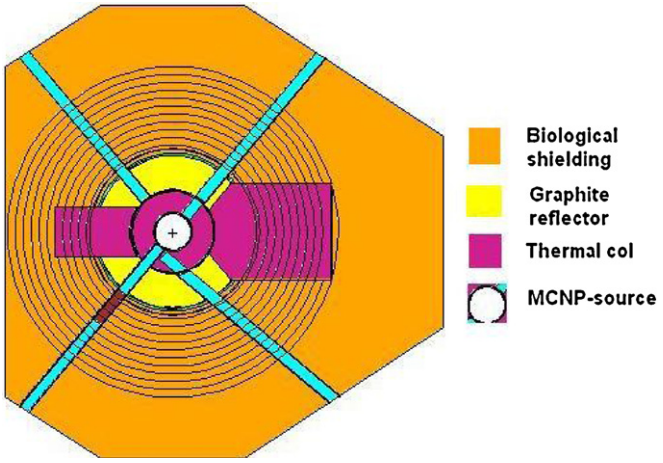

Fig. 4. Top (or *XY*) view of the MCNP extended model of the TRIGA reactor.

It is recognized that the convergence of MC calculation for large-scale systems is very time-consuming or even not achievable. The accurate and complete information for the individual MC particle tracks are required in order to perform good quality calculations. The MCNP computer code provides a Surface Source Writing (SSW) capability to generate a WSSA-format file which contains all required messages of individual particle tracks crossing a given surface (MC team, 2005).

The SSW capability is applied not only to reduce the computational cost but also to perform good calculations because it incorporates complete and accurate information of each individual MC particle crossing the source surface. In the MC simulation, the particle tracks of interest crossing this surface are recorded in the WSSA-format file (Chen and Fischer, 2005). The execution of the model first needs to run with SSW card to generate WSSA file. Then, the second execution is performed with SSR card and by changing the name of WSSA by RSSA file. This source-file contains all required messages of individual particle tracks crossing a given surface.

On an extended model execution, it is seen at the output that the tracks entering into the cells are decreased and vanished in bulk biological shielding cell. This situation also creates very bad statistics. Therefore, to solve this problem, MCNP provides several techniques that can be tried to solve this problem, one obvious solution is to run more particles, but computationally it is very expensive. Avoiding the computational cost by the brute force approach of running more particles, this model applies the variance reduction technique (Khan, 2010).

3.1. MCNP model of the thermal column

To calculate the thermal flux density, superimposed mesh FMESH tally is invoked into the extended model. The FMESH card allows the user to define a mesh tally superimposed over the problem geometry. Results are written to a separate output file with the default name MESHTAL. By default, the mesh tally estimates the track length of the particle flux density, averaged over a mesh cell, in units of particles/cm^2, and is normalized to "per starting particle", except in KCODE criticality calculations (MC team, 2005).

For thermal flux density analysis, FMESH is applied to one face of the thermal column where measurements are performed at 13 different positions. The coarse mesh for each position is selected so that one graphite block is represented by one tally mesh. The MCNP5 model of thermal column is shown in Fig. 6. Each point of measurement (as shown in Fig. 7) is marked with plus sign i.e."+". The mesh tally is applied to (11×11) matrix of the thermal column excluding the upper most and lower most graphite layers. The

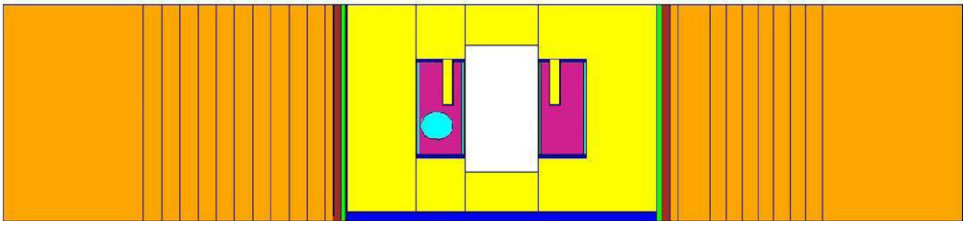

Fig. 5. Side (or *YZ*) view of the complete MCNP model of the TRIGA Mark II reactor.

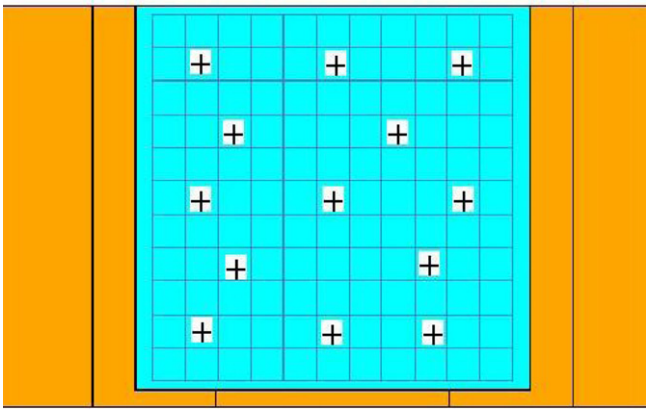

Fig. 6. The MCNP model of the thermal column.

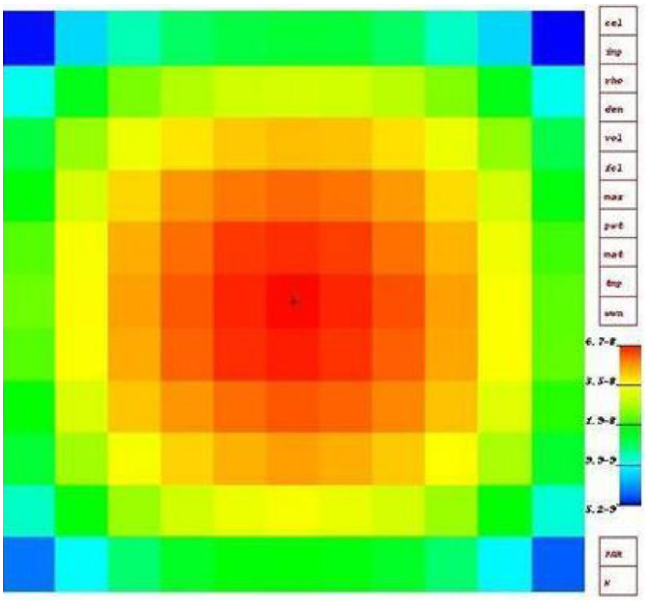

Fig. 7. MESH tally plot of the thermal column of the reactor.

thermal flux density is measured on (2 × 2), (2 × 6), (2 × 10), (4 × 3), (4 × 8), (6 × 2), (6 × 6), (6 × 10), (8 × 3), (8 × 9), (10 × 2), (10 × 6) and (10 × 10) positions and compared with corresponding MCNP calculations.

The model is run on source size (NPS) 1.0E+7 with Surface Source Reading (RSSA) file. The MCNP MESH tally plot of thermal column is given in Fig. 7.

3.2. MCNP model of the beam tube-A

The extended model is modified for BT-A experiment described in Section 2.2. The barite concrete compositions of measuring barrel and TRIGA bulk shielding have been applied to the model (Krejci, 2007; Williams et al., 2006). To calculate the thermal flux density in the BT-A, a mesh tally is utilized. The MCNP model of BT-A is shown in Fig. 8. The simulated results are given in units of particles per cm^2 at the output file MESHTAL. These results are normalized to the first experimental point to convert the MCNP results into real flux density units.

4. Discussions of the results

4.1. Thermal column

The extended MCNP model is applied to the experimental thermal flux density at selected positions in the thermal column. The experimental observations are compared with those of theoretical predictions in Table 2. Each gold foil was measured three times and an average value is used. The theoretical and experimental relative error for each selected position is also given in Table 2. Both experimental and theoretical results are agreed on the fact that the thermal flux density is maximum at the centre and decreases in the radial direction. It is also agreed that flux density in the upper part of the thermal column is smaller than in the lower part. This difference may be attributed to the fact that all three control rods are mostly kept in upper part of the reactor core during the reactor operation and depress the flux density in the upper part. Thus both i.e. MCNP and experimental results show the influence of control rods. The one possible justification between the theoretical and experimental deviations is the difference in the material structure and composition of the thermal column. The actual block structure of the thermal column is approximated as uniform and homogenous graphite in the thermal column. The second possible justification is that experiment measures all neutrons entering into the foil which is not 100% cadmium covered while the model simulates all neutrons below 0.4 eV. The model uses 0.4 eV as cadmium cut off and actual cut off may vary from 0.4 eV.

4.2. Beam tube A

This experiment was performed in different environment than the thermal column experiment. The thermal flux density is measured in the BT-A employing gold foil activation method. The MCNP extended model of the reactor is applied to these measurements. The experimental results are compared with the MCNP calculations in Fig. 9 and Table 3. Both, the theoretical and experimental results are agreed that the thermal flux density has decreasing trend along the BT-A length. Fig. 9 shows that both MCNP and experimental values on the front face (refers to point no. 0) of the BT-A are higher than the next points values (i.e. at 12 cm, 24 cm, etc.). It may be due to the high neutron reflection from the front face of concrete barrel. The possible justification of the deviations between measurements and calculations is the difference of material composition of the barite concrete applied to biological shielding of the MCNP model. The standard barite concrete (Williams et al., 2006)

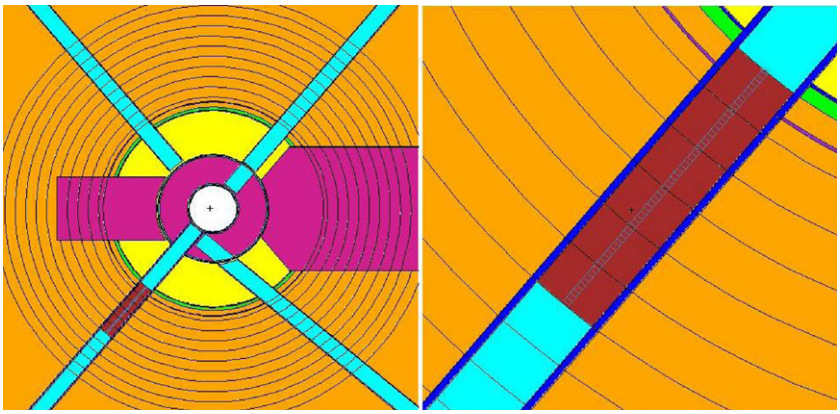

Fig. 8. MCNP extended model (left) and MESH applied BT-A model (right).

Table 2
Experimental and theoretical thermal flux density in the thermal column.

Measurement positions	Exp. thermal flux (#/cm^2 s)		Cal. thermal flux (#/cm^2 s)		Cal./Exp.
	Value	Rel. error	Value	Rel. error	
(2,2)	1.6932E+07	5.20	2.0755E+07	2.74E−02	1.226
(2,6)	1.9255E+07	6.08	3.7084E+07	1.89E−02	1.926
(2,10)	1.5848E+07	2.65	2.0693E+07	2.74E−02	1.306
(4,3)	4.5127E+07	6.08	5.0593E+07	2.13E−02	1.121
(4,8)	5.6064E+07	6.24	6.0810E+07	1.78E−02	1.085
(6,2)	2.9609E+07	3.61	4.4650E+07	2.13E−02	1.508
(6,6)	8.3050E+07	3.46	8.3050E+07	1.72E−02	1.000
(6,10)	4.5768E+07	5.29	4.4126E+07	1.97E−02	0.964
(8,3)	4.4985E+07	4.36	5.2957E+07	2.00E−02	1.177
(8,9)	4.4196E+07	4.00	6.3907E+07	1.81E−02	1.446
(10,2)	2.0561E+07	3.00	2.2168E+07	2.48E−02	1.078
(10,6)	3.2400E+07	4.00	4.2623E+07	1.97E−02	1.315
(10,10)	1.6723E+07	3.00	2.2406E+07	3.01E−02	1.340

Table 3
The comparison of thermal flux density in the BT-A.

Barrel length (cm)	Exp. thermal flux (#/cm^2 s)		Cal. thermal flux (#/cm^2 s)		Exp./Cal.
	Results	%-error	Resuts	Rel. error	
0	6.94E10	0.2	6.94E10	4.27458E−02	1.00
12	2.03E10	0.4	1.72E10	9.67595E−02	1.18
24	6.59E09	0.7	3.81E09	1.51364E−01	1.70
36	2.20E09	1.0	1.09E09	1.65035E−01	2.00
48	7.25E08	1.5	1.86E08	2.59576E−01	3.80
60	2.65E08	1.9	1.14E08	3.05689E−01	2.32

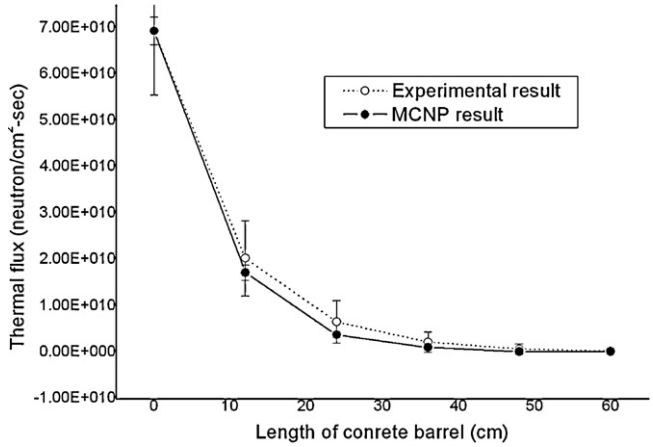

Fig. 9. Thermal flux density in the BT-A of the reactor.

is used in the model while the actual concrete composition needs its experimental investigation.

The experimental values at the selected measuring points are higher than theoretical results. It may be because of the additional irradiation of foil before the reactor reaches its full power because during the reactor start up, the reactor power is increased in steps to reach the full power. Similarly the reactor also takes some time to go from full power to reach shutdown condition. The experiment measures the total irradiation from the start up to completely shut down state while model only calculates irradiation at full power.

4.3. Diffusion length

The diffusion length is one of the important neutrons shielding parameter which depends on the thickness of the material and the energy of the neutron. The diffusion length of thermal neutron in the barite concrete is calculated by using the following relation

(Shultis and Faw, 2000)

$$\Phi_l = \Phi_0 \exp\left(-\frac{l}{d}\right)$$
$$\Rightarrow d = -\frac{l}{\ln(\Phi_l/\Phi_0)}$$

where d is diffusion length, l is the length of the concrete barrel; Φ_l is the flux density at length l and Φ_0 shows the flux density at the front face of the barrel. The experimental and theoretical diffusion lengths are determined as 10.77 cm (Krejci, 2007) and 9.36 cm respectively with a difference of 13%. This deviation may be due to the difference composition and structure between theoretical and actual barite concrete.

5. Conclusion

The shielding parameters outside the TRIGA reactor core are calculated using an extended MCNP model of the TRIGA Mark II reactor biological shielding. The theoretical values are verified experimentally in the thermal column and one of the beam tubes (i.e. BT-A) region. The extended model does not incorporate an accurate model of the radiographic collimator. Since it is very close to BT-A and requires its correct modeling. The standard barite material composition is applied to the model which could be slightly different than the actual composition. Therefore this computational model of the reactor can further be improved by incorporating the accurate model of the radiographic collimator and original material composition of the biological shielding.

References

Böck, H., 1996. Sicherheitsbericht für das Atominstitut der Österreichischen Universitäten. Safety Analysis Report for the Atominstitute, TU-Vienna, Atominstitute AIAU 96301, Vienna, Austria.

Chen, Y., Fischer, U., 2005. Program system for three-dimensional coupled Monte Carlo-deterministic shielding analysis with application to the accelerator-based IFMIF neutron source. Nuclear Instruments and Methods in Physics Research A 551, 387–395 (2005).

General Atomics (GA), 1962. 100-kW TRIGA MARK II Pulsing Reactor Mechanical Maintenance and Operational Manual, GA, USA (Chapter 3).

Karimzadeh, S., 2004. Behaviour of the electronic seals in mixed radiation fields. MS Thesis, Atominstitute, Vienna University of Technology, pp. 20–22.

Khan, R., 2010. Neutronics Analysis of TRIGA Mark II research reactor and its facilities. PhD Thesis, Atominstitute, Vienna University of Technology, Vienna, Austria.

Krejci, D., 2007. Messung der Neutronendiffusionslnge in Schwerbeton, No. AIAU 27305. Atominstitute of Vienna University of Technology.

X-5 Monte Carlo team, 2005. A General Monte Carlo N-Particle Transport Code, Version 5. MCNP5 Manual. Los Alamos National Laboratory, USA.

Shultis, J.K., Faw, R.E., 2000. Radiation Shielding. La Grangré Park, IL, USA, pp. 304–307, ISBN 0-89448-456-7.

Williams III, R.G., Gesh, C.J., Pagh, R.T., 2006. Compendium of Material Composition Data for Radiation Transport Modelling. Pacific Northwest National Laboratory, pp. 14–18.